Normal-Incidence Mid-Infrared Ge Quantum-Dot Photodetector

FEI LIU,[1,3] SONG TONG,[1] JIANLIN LIU,[2] and KANG L. WANG[1]

1.—Device Research Laboratory, Department of Electrical Engineering, University of California at Los Angeles, Los Angeles, CA 90095. 2.—Department of Electrical Engineering, University of California at Riverside, Riverside, CA 92521. 3.—E-mail: feiliu@ee.ucla.edu

Mid-infrared photodetectors were demonstrated by using molecular-beam epitaxy (MBE)-grown self-assembled Ge quantum dots (QDs). The response wavelength ranged from 2.2 μm to 3.1 μm and peaked at 2.8 μm. The peak response wavelengths shifted to 2.9 μm and 3.5 μm after thermal annealing at 700°C and 900°C for 5 min, respectively. Normal-incidence detection was confirmed, and the mechanism of a Ge QD photodetector was discussed. Calculations showed the key parameters determining response wavelength of the Ge QD infrared photodetector, which agreed with experimental results.

Key words: Ge quantum dot (QD), mid-infrared photodetector, annealing

INTRODUCTION

The 3–5-μm and 8–12-μm wavelength ranges are important windows for infrared detector applications because of low atmospheric loss in these regions. Because of its proper bandgap energy, mercury cadmium tellurium (HgCdTe) photodetectors have been developed for these wavelength ranges.[1] On the other hand, intensive studies have been carried out for photodetectors with III-V substrates, such as GaAs and InP, by exploiting quantum wells (QWs) or quantum dots (QDs), referred to as quantum-well infrared photodetector (QWIP) and quantum-dot infrared photodetector (QDIP). There are advantages of using QDs. For QWIPs, such as AlGaAs/GaAs, using conduction intersubband transitions,[2,3] normal-incidence absorption is forbidden because of the intersubband transition selection rule.[4] However, by using QDs such as InAs or InGaAs dots, as the absorption region, normal-incidence response can be, in principle, obtained because of the lateral quantum confinement.[5–7] Furthermore, lower photoconductive loss is anticipated because of the reduced capture probability of photogenerated carriers by the dots.[8] However, to integrate with a Si integrated circuit monolithically, Si-based devices are preferred. Because of the large discontinuity in the SiGe/Si valance band, the intervalence subband transitions of holes from the ground state of the dots to the continuum states can be used for infrared detectors working in mid-infrared wavelength regions.[9] The SiGe/Si photodetectors can be monolithically integrated on Si substrates with complementary metal-oxide semiconductor (CMOS) readout circuits, making low cost devices possible. After the observation of the intersubband transition in the Ge QDs,[10] progress has been made on the fabrication of Ge QD mid-infrared photodetectors.[11–13] Absorption spectra were measured for infrared photodetectors with lateral and vertical carrier transport. In this paper, the experimental results of annealing Ge QD mid-infrared photodetectors will be presented. The normal-incidence absorption mechanism is discussed. Calculations show the peak-response wavelength dependence for SiGe QDIPs, which can be used to explain the anneal effects for the Ge dot mid-infrared photodetector.

(Received October 11, 2003; accepted April 8, 2004)

EXPERIMENTS AND RESULTS

The detector structure was grown at 540°C by solid-source molecular-beam epitaxy (MBE) on a double-side-polished Si (100) wafer with a boron doping of 1×10^{19} cm^{-3}. The wafer was chemically cleaned immediately before being introduced into the MBE chamber. The active region consisted of 20 periods of boron-doped Ge QD layers separated by 20-nm Si barriers. The Ge dots were grown under the Stranski–Krastanov mode. The nominal Ge-layer thickness was 1.5 nm. A transmission electron microscopy (TEM) image showed that the sample had Ge dots with an average of 9 nm in height and an average of 100 nm in width. The doping density

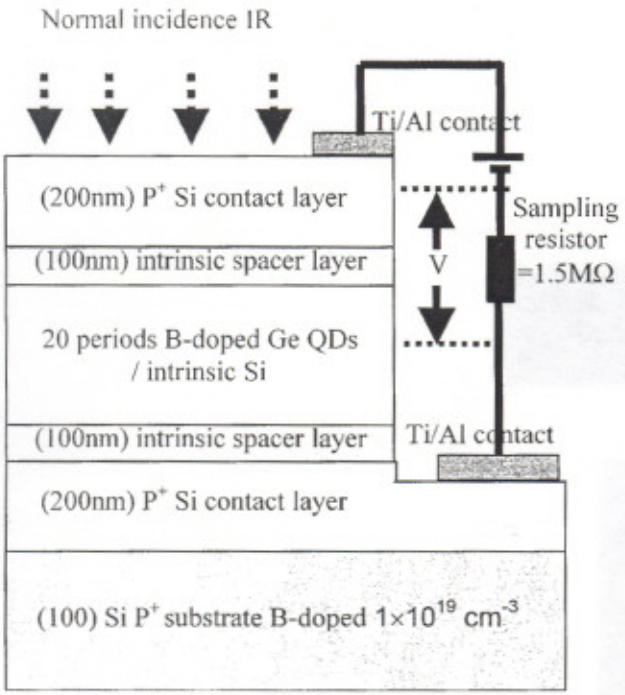

Fig. 1. Schematic drawing of a mesa-type Ge dot photodetector. The active layer consists 20 periods of boron-doped Ge QD layers separated by 20-nm Si barriers.

for the Ge layers was about 6×10^{18} cm^{-3}. The active-dot superlattice region was embedded in two Si intrinsic-spacer layers (100 nm) from the P^+ Si contact layers (200 nm). Mesa-type photo-detectors were fabricated by standard photolithography. E-beam evaporated Ti/Al films followed by 1-min annealing at 450°C were used as contacts. Figure 1 shows the schematic drawing of the photodetector. To achieve 3–5-μm detection, a postgrowth thermal process was used to tune the response wavelength.

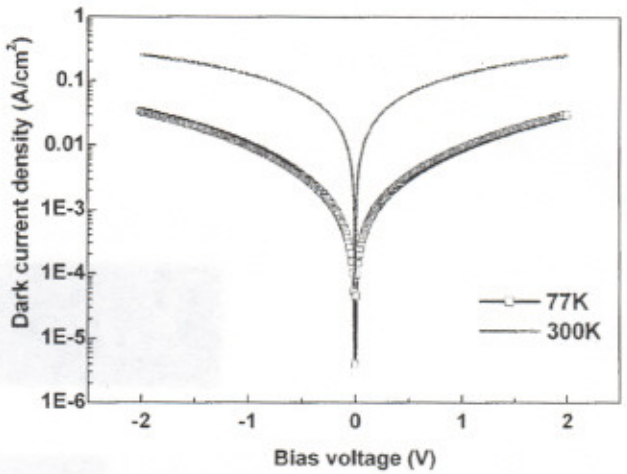

Fig. 2. The current-voltage characteristics of the as-grown sample measured at 77 K and 300 K.

Two samples were annealed at 700°C and 900°C in nitrogen for 5 min.

The current-voltage characteristics of the as-grown sample at both 77 K and 300 K were shown (Fig. 2) to be nearly symmetric for positive and negative biases, indicating that the p-i-p structure had symmetric doping. A relatively large dark-current density was due to high doping density in the QDs.[14] Assuming that the doping density in the Ge dots is the same as the Ge layer, it was estimated, from the dimension of the QDs, that there were roughly 60 holes in each Ge dot. The large number of holes in a dot is due to the high doping density and the large Ge dots, especially in the lateral dimension.

Normal-incidence photocurrent spectra of the sample were measured at 80 K using a lock-in amplifier through a sampling resistor (R = 1.5 MΩ). As shown in Fig. 3a, the intensity increased when the

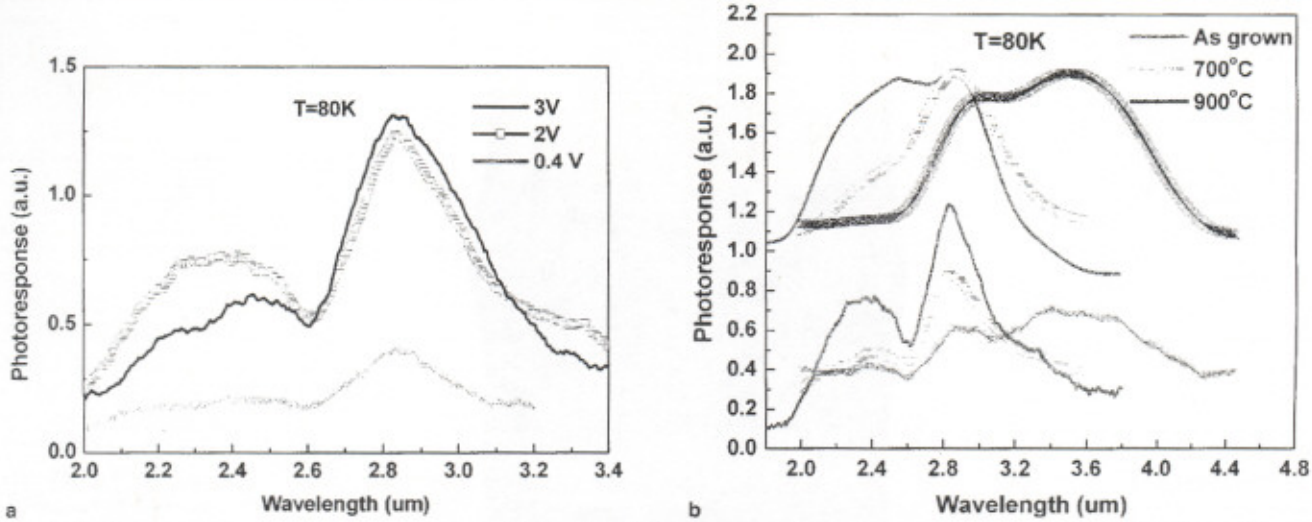

Fig. 3. Photoresponse spectra of as-grown and annealed samples. (a) Response spectra of the as-grown sample at 80 K with different biases. The peak-photoresponse wavelength occurred at 2.8 μm. (b) Response spectra of the as-grown sample, 700°C annealed sample, and 900°C annealed sample at 80 K, showing a redshift for the peak photoresponse. The lower three curves were the measured spectra, and the upper three curves were the normalized spectra obtained by dividing the measured spectra with the atmospheric absorption spectrum.

bias voltage was increased from 0.4 V to 3 V, which was due to a more efficient collection of the photoinduced carriers at higher biases. The peak response saturated with increasing bias because of relatively small diode resistance at large bias. The response peak of this sample occurred at around 2.8 μm, corresponding to 443 meV, i.e., the energy from the ground state of the dots to the continuum states. For the sample annealed at 700°C, the peak photoresponse shifted to 2.9 μm; and for the 900°C annealed sample, the peak shifted to around 3.5 μm (Fig. 3b). However, the photoresponse intensity was reduced with annealing. In addition to these peaks, the photocurrent spectra of all these samples showed two dips at 2.6 μm and 3.1 μm. These were due to the absorption such as H_2O and CO_2 in the atmosphere. The three upper curves showed the normalized spectra by using measured spectra dividing the atmospheric absorption spectrum.

DISCUSSION

Absorption coefficient α is proportional to the momentum matrix element $M_{if} = \langle f|\hat{e}\cdot\vec{P}|i\rangle$, where i and f are the initial and final state wavefunctions, $\vec{P}$ is the momentum operator, and $\hat{e}$ is the light polarization direction. This indicates that the absorption coefficient depends on light polarization. To obtain normal-incidence absorption, the momentum matrix element for normal incidence must not vanish. If the QDs were sufficiently small, quantum confinement in the lateral direction can contribute to normal-incidence absorption. However, in many cases, i.e., self-assembled QDs, the QDs are flat and are more appropriately to be described as quasi-QWs or quantum discs, and thus, quantum confinement in the lateral direction is very weak and not sufficient to contribute normal-incidence absorption. Therefore, the normal-incidence photoresponse of the present Ge-dot photodetectors is not due to lateral quantum confinement. For our detector, the intersubband transitions occur in the valence band. The absorption mechanism in valence intersubbands is different from that in conduction intersubbands because of the p-like valence-band states. The heavy-hole states, light-hole states, and split-off states near the valence-band edge can be described as the following:

$$\phi_{hh} = -\frac{1}{\sqrt{2}}(|x\rangle + i|y\rangle)\uparrow \text{ or } \phi_{hh} = \frac{1}{\sqrt{2}}(|x\rangle - i|y\rangle)\downarrow$$

$$\phi_{lh} = -\frac{1}{\sqrt{6}}[(|x\rangle + i|y\rangle)\downarrow -2|z\rangle\uparrow]$$

$$\phi_{lh} = \frac{1}{\sqrt{6}}[(|x\rangle - i|y\rangle)\uparrow +2|z\rangle\downarrow]$$

$$\phi_{so} = -\frac{1}{\sqrt{3}}[(|x\rangle + i|y\rangle)\downarrow + |z\rangle\uparrow]$$

$$\phi_{so} = -\frac{1}{\sqrt{3}}[(|x\rangle - i|y\rangle)\downarrow - |z\rangle\uparrow]$$

where z is the growth direction.

In our detector, HH1 heavy hole ground state (is the ground state of QDs). The matrix elements, $M_{if} = \langle \phi_{lh}|\hat{e}\cdot\vec{P}|\phi_{hh}\rangle$ and $M_{if} = \langle \phi_{so}|\hat{e}\cdot\vec{P}|\phi_{hh}\rangle$ do not vanish for normal-incidence light. This means that normal-incident light can excite a heavy hole to light-hole transition or a heavy hole to split-off transition in this kind of Ge-dot intersubband photodetectors. To have photocurrent, photogenerated holes need to be collected by contacts; only those holes excited to the final continuum states can be efficiently collected to generate photocurrent. Otherwise, thermal excitations or tunneling are needed for the carriers to reach the continuum states and subsequently be collected. Thus, the normal-incidence mechanism for the present detector is due to the transition from the ground heavy-hole state to the light-hole or split-off continuum state. In this discussion, we assume that strain present in the dots does not change the selection rule. In reality, the characteristics of the valence-band wave functions are probably mixed from all the valence bands, and normal-incidence transitions in the same band may be possible. A preliminary quantitative analysis has been done, and the results indicate that the band mixing has significant contributions to normal-incidence detection. It is, however, interesting to note that absorption measurements in a waveguide geometry seem to show that the "heavy hole" to "heavy hole" transition in the case of strained SiGe and Si QWs still has the transition rule of the same band, i.e., $\cos^2\theta$.[15]

Usually, the more sophisticated eight-band k*p model has been used for absorption calculation, but here, we used a much simpler model because we only discuss the dependence of peak-response wavelength. We calculated response-wavelength dependence on dot parameters, i.e., QD height, width, Ge content and strain. As discussed previously, the optical transitions are mainly from the HH1 to continuum states, corresponding to the energy from the ground heavy-hole state to the potential edge. To evaluate the energy levels, a three-dimensional box, valence-band, finite-potential well model with effective mass approximation was used. Because QDs are partially relaxed,[16] the strain ratio $\frac{a_{//dot} - a_{si}}{a_{SiGe} - a_{si}}$ is used to describe the percentage of strain in QDs. Effective masses of SiGe dots at different Ge contents were obtained by Vegard's law $\frac{1}{m^*_{SiGe}} = \frac{x}{m^*_{Ge}} + \frac{1-x}{m^*_{Si}}$. For SiGe alloy materials, the changes of effective mass caused by strain was considered by using a two-band k*p method. Using the fully strained and full relaxed SiGe on Si-substrate band-offset data[17] and the strain ratio concept, the valence-band offset energies of partially strained $Si_{1-x}Ge_x$ layers on (100) Si substrate were obtained.

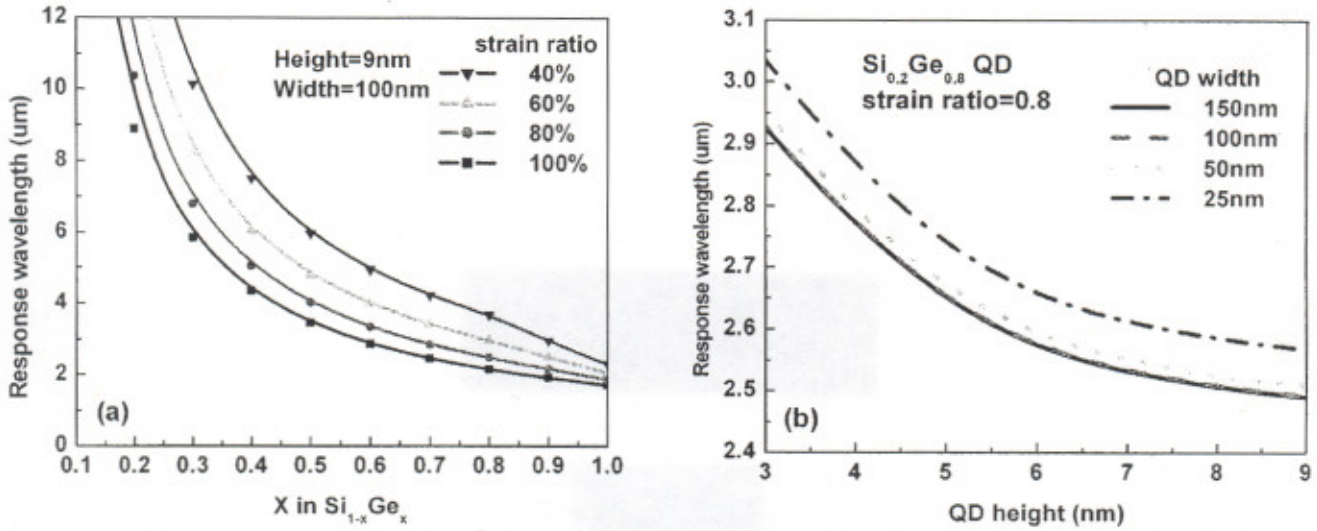

Fig. 4. Calculated peak-response wavelength. (a) Peak-response wavelength dependence on the Ge content and Ge QD strain ratio for the Ge QDs 9 nm in height and 100 nm in base. (b) Dot-dimension dependence of peak response for $Si_{0.2}Ge_{0.8}$ QDs with a strain ratio of 0.8.

Figure 4a shows the calculated results of response-wavelength dependences on $Si_{1-x}Ge_x$ x content and strain ratio for SiGe dots 9 nm in height and 100 nm in width. The calculations show that for longer wavelength response, lower Ge content in QD and smaller QD strain ratio are needed. These can be understood physically because the lower Ge content and smaller QD strain ratio make the valence-band offset smaller, so the transition energy from the heavy-hole ground state to continuum states becomes smaller, and hence, a longer response wavelength is obtained. Figure 4b shows the results of the response wavelength dependence on the QD dimensions at a constant strain ratio of 0.8 for the $Si_{0.2}Ge_{0.8}$ QD. For a smaller size of QD, the ground-state energy is higher (far away from the well bottom) because of the greater quantum-confinement effect. The peak wavelength changes about 16% as the dot height increases from 3 nm to 9 nm. Varying width dimension changes response wavelength slightly because of the relatively large width dimension compared to the height of the QDs.

As shown previously, the response of the as-grown sample ranged from 2.2–3.1 μm, while for the 700°C annealed one, the range shifted to 2.4–3.3 μm, and for 900°C annealed one, the range shifted to 2.7–4.1 μm. The annealing effect on response wavelength can be explained from some of the results of previous experiments[18,19] and calculations. One effect of annealing is the interdiffusion of Ge and Si, i.e., the Ge content in the QD decreases as annealing temperature and time increase. Another effect is that heat treatment makes the QDs relax more, and the strain ratio becomes smaller. Both effects lead to a smaller valance-band offset, and the response shifts to longer wavelength. The third effect is the QD becomes larger, and this will give shorter wavelength response. However, the calculations show that the QD dimension has a relatively smaller effect on the response wavelength for QDs with a height of 9 nm compared to the effects of Ge content and QD strain-ratio parameters. It should be pointed out that an eight-band k*p calculation seems to suggest that smaller QDs of pyramid shape give rise to normal-incidence absorption.[20] It also shows that the normal-incidence absorption coefficient will decrease when Ge content decreases.[20] The reduced intensity of the normal-incidence absorption caused by annealing can be explained because of the reduced Ge content and larger Ge dots.

For $Si_{1-x}Ge_x$, varying x composition and QD strain ratio is effective to change response wavelength. To obtain 3–5-μm photoresponse, we should have a lower Ge content in the dots, perhaps, by growing Ge QDs at higher temperatures. However, postgrowth thermal treatment (annealing) is an alternative way to change the response wavelength for intersubband transition photodetectors.

CONCLUSIONS

Normal-incidence response of the intersubband transition for a self-assembled Ge-dot detector was measured. The response ranged from 2.2 μm to 3.1 μm. Annealing shifted the peak response range to a longer wavelength, i.e., from 2.7 μm to 4.1 μm for the 900°C, 5-min annealed sample, and a peak response wavelength at 3.5 μm was identified for this annealed sample. The normal-incidence detection mechanism for the Ge QD photodetector was due to the transitions from the heavy-hole ground states to the light-hole or the spilt-off continuum states. Response-wavelength calculations gave the guides to design the Ge QDIPs at a certain response wavelength. Experimental results and calculations gave further understandings of annealing effects and showed that annealing is a convenient and effective way to tune the response wavelength. This work suggests that intersubband photodetectors using

Ge QDs on a Si substrate have potential applications for mid-infrared photodetectors.

ACKNOWLEDGEMENT

This work was supported in part by MURI and DMEA/DARPA.

REFERENCES

1. J.F. Siliquini and L. Faraone, *Semicond. Sci. Technol.* 11, 1906 (1996).
2. J.S. Smith, L.C. Chiu, S. Margalit, A. Yariv, and A.Y. Cho, *J. Vac. Sci. Technol. B* 1, 376 (1983).
3. B.F. Levine, *J. Appl. Phys.* 74, R1 (1993).
4. H.C. Liu, M. Buchanan, and Z.R. Wasilewski, *Appl. Phys. Lett.* 72, 1682 (1998).
5. S. Maimon, E. Finkman, G. Bahir, S.E. Schacham, J.M. Garcia, and P.M. Petroff, *Appl. Phys. Lett.* 73, 2003 (1998).
6. L. Chu, A. Zrenner, G. Bohm, and G. Abstreiter, *Appl. Phys. Lett.* 75, 3599 (1999).
7. Q.D. Zhuang, J.M. Li, H.X. Li, Y.P. Zeng, L. Pan, Y.H. Chen, M.Y. Kong, and L.Y. Lin, *Appl. Phys. Lett.* 73, 3706 (1998).
8. V. Ryzhii, *Semicond. Sci. Technol.* 11, 759 (1996).
9. K.L. Wang and R.P.G. Karunasiri, *Semiconductor Quantum Wells and Superlattices for Long-Wavelength Infrared Detectors*, ed. M.O. Manasreh (Boston, MA: Artech House, 1993), pp. 139–204.
10. J.L. Liu, W.G. Wu, A. Balandin, G.L. Jin, and K.L. Wang, *Appl. Phys. Lett.* 74, 185 (1999).
11. C. Miesner, O. Rothig, K. Brunner, and G. Abstreiter, *Appl. Phys. Lett.* 76, 1027 (1999).
12. A.I. Yakimov, N.P. Stepina, A.V. Dvurechenskii, and A.I. Nikiforov, *Phys. Rev. B* 63, 045312 (2001).
13. S. Tong, J.L. Liu, J. Wan, and K.L. Wang, *Appl. Phys. Lett.* 80, 1189 (2002).
14. V. Ryzhii, V. Pipa, I. Khmyrova, V. Mitin, and M. Willander, *Jpn. J. Appl. Phys.* 39, 1283 (2000).
15. K. Boujdaria, S. Ridene, S.B. Radhia, O. Zitouni, H. Bouchriha, and G. Fishman, *J. Appl. Phys.* 92, 2586 (2002).
16. Z.M. Jiang, X.M. Jiang, W.R. Jiang, Q.J. Jia, W.L. Zheng, and D.C. Qian, *Appl. Phys. Lett.* 76, 3397 (2000).
17. M.M. Rieger and P. Vogl, *Phys. Rev. B* 48, 14276 (1993).
18. J. Wan, Y.H. Luo, Z.M. Jiang, G. Jin, J.L. Liu, K.L. Wang, X.Z. Liao, and J. Zou, *Appl. Phys. Lett.* 79, 1980 (2001).
19. X.Z. Liao, J. Zou, D.J.H. Cockayne, J. Wan, Z.M. Jiang, G. Jin, and K.L. Wang, *Appl. Phys. Lett.* 79, 1258 (2001).
20. Y.-Y. Lin and J. Singh, to be published in *J. Appl. Phys.*